RSC Advances

ROYAL SOCIETY OF CHEMISTRY

www.rsc.org/advances

Effects of PVDF/SiO_2 hybrid ultrafiltration membranes by sol-gel method for the concentration of fennel oil in herbal water extract

Xin Huang[1], Jing Zhang[1], Weiping Wang[1], Yaodong Liu[1], Zhibing Zhang[1], Lei Li[1*], Wenling Fan[2*]

1. Department of Chemical Engineering, School of Chemistry and Chemical Engineering, Nanjing University, Nanjing 210093, P.R.China

2. College of Pharmacy, Nanjing University of Chinese Medicine, Nanjing 210029, P.R.China

*** Corresponding Authors and their present address:**

1. Lei Li, Ph.D，Associate Professor.

Department of Chemical Engineering, School of Chemistry and Chemical Engineering, Nanjing University

22 Hankou Road, 210093 Nanjing, P.R.China

Tel: +86-025-83596665-810, +86-0-13813826914

Fax:+86-025-83593772

E-mail: lilei@nju.edu.cn; ll-nju@163.com

2. Wenling Fan, Ph.D，Associate Professor.

College of Pharmacy, Nanjing University of Chinese Medicine

138 Xianlin Rd., 210046 Nanjing, P.R.China

Tel:(+86)-0-13851796270

E-mail: fanwl.happy@163.com

Abstract

In this paper, organic-inorganic polyvinylidene fluoride (PVDF)/ silica (SiO_2) hybrid membranes were prepared via phase inversion by a tetraethoxysilane (TEOS) sol-gel process and were used to concentrate fennel oil in herbal water extract. Such characteristics of the hybrid membranes as crystal structure, mechanical properties, thermal stability, morphology, hydrophilicity, and permeation performance were investigated thoroughly. The analytical results showed that the interaction existed between SiO_2 nanoparticles and PVDF polymers, and that the thermal and mechanical properties of the hybrid membranes were improved by the introduction of SiO_2. Besides, the crystalline structure of PVDF changed from β phase to α phase when TEOS content surpassed 20%. Furthermore, the experimental data indicated that hydrophilicity, permeation, rejection, porosity and mean pore size of the hybrid membranes also increased with ascending TEOS contents, but higher TEOS contents had negative effect on those properties. Finally, the concentration process of fennel oil in herbal water extract through the hybrid membranes was conducted and it proved that the separation performance was effectively improved.

Keywords: extract; fennel oil in water; polyvinylidene fluoride; silica; sol-gel method; ultrafiltration;

1. Introduction

Every year, a huge volume of water extract containing herbal volatile oil is produced from various industrial sites such as the pharmaceutical and food industry, which need to be purified and concentrated. Conventional separation methods of volatile oil in water extract such as gravity separation and skimming, air-flotation, coagulation, de-emulsification and flocculation, have the intrinsic disadvantages such as low efficiency, high operation cost, corrosion and re-contamination problems. Several studies have been reported on the use of ultrafiltration membranes for the treatment of oil-in-water emulsions [1-3]. The pore size of ultrafiltration membrane is usually in the range of 0.002-0.15 μm, whilst the size of the oil droplets in emulsion is usually in the range of 0.08-10 μm. Therefore, most of these oil droplets can be effectively removed. [4].

Polyvinylidene fluoride (PVDF) has been used extensively in ultrafiltration membrane processes, such as wastewater treatment and protein effluent separation [5, 6]. However, it has to confront severe membrane fouling and decline of permeability due to its strongly hydrophobic

nature, which has been a barrier to its application. Many studies have attempted to improve the performance of PVDF membranes using various techniques, including chemical grafting, physical blending, and surface modifications [7-12]. Among those methods, blending with inorganic materials has been paid more and more attention. This is attributed that composite materials can combine basic properties of organic and inorganic materials and offer specific advantages for the preparation of artificial membranes with excellent separation performances, good thermal and chemical stability and adaptability to the harsh environments, as well as membrane forming ability.

Inorganic additive materials for polymeric membranes include silica [13-15], zirconium dioxide (ZrO_2) [16], aluminium oxide (Al_2O_3) [17], titanium dioxide (TiO_2) [18, 19] etc. Among various nanoparticles, silica is the most convenient and widely used because of its mild reactivity and well-known chemical properties [20-22]. An easy way of preparing organic-silica hybrid membranes is sol-gel technique. It can introduce inorganic frameworks into polymers by the hydrolysis and condensation reaction of tetraethoxysilane (TEOS) [23-27], which results in improved chemical, mechanical, and thermal stability without significant decrease in the transport properties of the polymers.

This work aims to prepare PVDF/SiO_2 hybrid ultrafiltration membranes by sol-gel method. The effects of SiO_2 nonoparticles on membrane properties such as pure water flux, BSA rejection, mean pore size, porosity, hydrophilicity, thermal analysis, mechanical analysis and surface analysis were studied systematically and thoroughly. Furthermore, the concentration process of fennel oil in water, typically representative of herbal water extract, was carried out through PVDF/SiO_2 hybrid membranes to validate effective improvement of ultrafiltration performance.

2. Experimental

2.1. Materials

PVDF (FR904, molecular weight (MW) =380,000) was purchased from Shanghai 3F New Materials Company, China. *N, N*-dimethylacetamide (DMAc), polyethylene glycol with MW of 400 (PEG400), ethanol, tetraethoxysilane (TEOS) were of analytical grade and obtained from Sinopharm Chemical Reagent Company, China. Bovine serum albumin (BSA, MW = 67,000) was gained from Shanghai HuiXing Biochemistry Reagent Company, China. Hydrochloric acid (HCl, 37wt.%) was of analytical grade from Nanjing Chemical Reagent Company. Ultrapure water was produced by a Millipore direct-Q system. All other chemicals used in the experiments were all of

analytical grade and used without further purification.

2.2. Membrane Preparation

2.2.1. Preparation of unfilled PVDF membrane

Unfilled PVDF membranes were prepared by the phase inversion method. A casting solution was obtained by dissolving PVDF powder (10 wt.%) and PEG400 (4 wt.%) in DMAc with vigorous stirring for 12 h at 60 ℃ and was kept quietly in the dark afterward for 2-3 days to remove air bubbles. Then a self-made scraper was used to cast the solution on a clean glass plate to get wet membranes. The wet films were kept in air for 30s and then immerged into ethanol/water (1/5, v/v) bath at 20±1 ℃ to complete phase inversion. Then those membranes prepared were immersed in deionized water for 24 h and the thickness of membranes was determined as about 200 μm by Dial Thickness Gauge (Peacock, Ozaki MFG. Co., Ltd. Japan). The unfilled PVDF membrane was marked as PT0.

2.2.2. Preparation of PVDF/SiO_2 hybrid membrane by sol-gel process

PVDF polymer (10 wt.%) and PEG400 (4 wt.%) were dissolved in DMAc with vigorous stirring for 12h at 60 □ to obtain homogeneous PVDF solution. The clear TEOS solution was obtained by mixing deionized water, hydrochloric acid (37wt.% HCl), ethanol and TEOS according to a molar ratio of 2:0.01:7:1. Then four mixtures with such various weight ratios of PVDF to TEOS as 9:1, 8:2, 7:3 and 6:4 were obtained by adding different amounts of TEOS solution into the above PVDF solution. The following preparation steps were the same as the unfilled PVDF membranes. The hybrid membranes prepared above were marked as PT10, PT20, PT30 and PT40, respectively.

2.3. Membrane characterization

The crystalline properties of the membranes were investigated by a X-ray diffraction (XRD)-6000 diffractometer (Rigaku, Japan) operated at 50mA and 50kV from 10°-50°. Before the test, the samples were dried overnight at 120 ℃ in a vacuum oven.

The chemical composition of the membranes was analyzed by Fourier transform infrared (FTIR) spectroscopy (Thermo Electron Corp., Nicolet 5700, USA).

Morphology and roughness of membranes were studied by atomic force microscopy (AFM) (Nanoscope III 710, Zeiss, USA) in air with tapping mode.

Differential scanning calorimetry (DSC) and thermal gravimetric analysis (TGA) were carried out for the evaluation of thermal stability of membranes with thermal analyzer (STA 449C, NETZSCH, Germany) under N_2 atmosphere at a heating rate of 10 □·min^{-1} from 30 □ to 700 □.

Tensile strength and elongation at break of membranes were determined by a universal mechanical testing instrument (Instron 4465, USA). Measurements were carried out at room temperature and a strain rate of 50 mm·min^{-1} was employed. For each membrane, at least three specimen tests were conducted.

Surface hydrophilicity of the membranes was determined by contact angle value of a drop of deionized water on the membranes surface using an OCA30 Contact Angle Meter (Dataphysics Instruments Gmb., Germany). To minimize experimental error, at least ten measurements at different sites of each sample were carried out and then the results were averaged.

The membrane porosity (ε) was defined as the volume of the pores divided by the total volume of the porous membrane. It was determined by gravimetric method and calculated by Eq. (1) [28]. Mean pore size (r_m) was determined by filtration velocity method. According to Guerout-Elford-Ferry equation, r_m could be calculated by Eq. (2) [29].

$$\varepsilon = \frac{W_1 - W_2}{\rho_w A L} \qquad (1)$$

$$r_m = \sqrt{\frac{(2.9 - 1.75\varepsilon) \times 8\eta L J}{\varepsilon \times A \times \Delta P}} \qquad (2)$$

where ε is the membrane porosity (%), W_1 is the weight of the wet membranes (g), W_2 is the weight of the dry membranes (g), ρ_w is the water density denoted as 0.998g·cm^{-3}, A is the effective area of the membrane (m^2), L is the membrane thickness (m), r_m is mean pore size (nm), η is the water viscosity denoted as 8.9×10^{-4} Pa·s, J is the permeation flux of the membrane for pure water (m^3.m^{-2}.s^{-1}), and ΔP is the operating pressure differential which is denoted as 0.2 MPa in this study.

2.4. Permeation property measurements

2.4.1. Pure water fluxes and rejection rate of BSA

The pure water flux and rejection rate of the membranes were measured by UF experimental equipment as described by Xu [30]. The obtained membrane sheets were cut into 10 cm diameter circles. The ultrafiltration process was operated under upstream pressure of 0.3 MPa with deionized

water for 5 h before the measurements. Then the upstream pressure was reduced to 0.2 MPa and the ultrafiltration experiments began. The stable pure water flux at the end of 1h was referred to as initial pure water flux (J_0) and calculated by Eq. (3).

Then 200mg/L BSA aqueous solution (pH 7.4, 0.01 M PBS buffer solution as a solvent) was selected as filtration solution instead of deionized water. At the end of 1h ultrafiltration, the permeate flux was considered stable. The BSA concentration in the feed and permeate samples were determined at the wave length of 280nm using UV/Vis spectrophotometer (UV752, ShangHai Youke Instrument Company, China). Rejection rate (R) was defined by Eq. (4).

$$J_0 = \frac{Q}{At} \qquad (3)$$

$$R = (1 - \frac{C_t}{C_0}) \times 100\% \qquad (4)$$

Where J_0 is the permeation flux of the initial membrane for pure water ($L \cdot m^{-2} \cdot h^{-1}$), Q is the volume of the permeate water (L), A is the effective area of the membrane (m^2), t is the permeate time (h), R is the rejection rate to BSA (%), Ct is the BSA concentration in the feed solution ($mg \cdot L^{-1}$) and C0 is the BSA concentration in the permeate solution ($mg \cdot L^{-1}$).

2.4.2. Anti-fouling property of membranes

After BSA ultrafiltration process, the membranes were washed with distilled water for 10 min and then the stable pure water flux through the cleaned membranes (J_t) was measured and calculated by Eq. (5). In order to evaluate the anti-fouling property of membranes, flux recovery (FR) was introduced and calculated by Eq. (6). All ultrafiltration experiments were conducted at room temperature.

$$J_t = \frac{Q}{At} \qquad (5)$$

$$FR = \frac{J_t}{J_0} \times 100\% \qquad (6)$$

where J_0 is the permeation flux of the initial membrane for pure water ($L \cdot m^{-2} \cdot h^{-1}$), J_t is the permeation flux of the cleaned membrane after fouled by BSA for pure water ($L \cdot m^{-2} \cdot h^{-1}$), Q is the volume of the permeate water (L), A is the effective area of the membrane (m^2), t is the permeate time (h) and FR is flux recovery (%).

2.5. The concentration process of fennel oil in water extract

2.5.1. Preparation and characterization of fennel oil in water extract

The fennel oil in 4 L water extract was prepared from 400 g fennel slices by steam distillation. The water extract was mixed by high-shear emulsifying dispersion for 20 min. The size of the oil droplets, which was measured using the dynamic light scattering measurements (Submicron Particle Sizer, Nicomp Model 370, Santa Barbara, Canada), was in the range of 0.1-0.3 μm with a volume average particle diameter of 0.2 μm.

2.5.2. Ultrafiltration separation of fennel oil in water extract

The concentration process of fennel oil in water extract was carried out by UF experimental equipment as described above. The obtained membrane sheets were cut into 10 cm diameter circle. The ultrafiltration process was operated under upstream pressure of 0.3 MPa with water extract for 5 h before the measurements. Then the upstream pressure was reduced to 0.2 MPa and the ultrafiltration experiments began. The stable flux of water containing fennel oil at the end of 1 h was referred to as initial flux of water containing fennel oil (J_{wf}) and calculated by Eq. (7). Considering that fennel oil consists of many concrete organic compounds, chemical oxygen demand (COD) values of the feed and permeate samples were determined by potassium dichromate standard method [31] and reflected the total organic concentration in fennel oil. Removal rate of COD (RR_{COD}) was defined by Eq. (8) and was used for evaluating the rejection effects of membranes to fennel oil.

$$J_{wf} = \frac{Q}{At} \qquad (7)$$

$$RR_{COD} = (1 - \frac{COD_p}{COD_f}) \times 100\% \qquad (8)$$

where J_{wf} is the permeation flux of water containing fennel oil ($L.m^{-2}.h^{-1}$), Q is the volume of the permeate water containing fennel oil (L), A is the effective area of the membrane (m^2), t is the permeate time (h), RR_{COD} is the removal rate of COD (%), COD_f is COD value of the feed samples, and COD_p is COD value of the feed and permeate samples.

3. Results and discussion

3.1. FTIR results

Fig. 1 showed the FTIR spectra of hybrid membranes (PT10, PT20, PT30 and PT40) and unfilled PVDF membranes (PT0). As seen in Fig. 1, the characteristic absorption bands for asymmetric Si-O-Si stretching and Si-OH stretching [32] appeared near 1048 cm^{-1}, 1162 cm^{-1} and 960 cm^{-1} in all hybrid membranes. It was known that PVDF crystallized in four different polymorphs (α, β, γ and δ) and each crystal structure had different polymorphs. Kim [33] reported that the FTIR absorption bands of PVDF was characteristic of such polymorphs as α（1384 cm^{-1}, 1211 cm^{-1}, 1150 cm^{-1}, 976 cm^{-1} and 766 cm^{-1}），β [34]（1274 cm^{-1} and 840 cm^{-1}），and γ [35]（815 cm^{-1}, 776 cm^{-1} and 430 cm^{-1}）. For PT0, PT10 and PT20 membranes, distinct β characteristic peaks at 1274cm^{-1} and 840 cm^{-1} could be observed. When TEOS content surpassed 30%, apparent α characteristic peaks at 1211 cm^{-1} and 766 cm^{-1} appeared for PT30 and PT40 membranes. The FTIR results showed that α-crystal formation of PVDF was changed into β-crystal formation due to redundant SiO_2 generated by sol-gel.

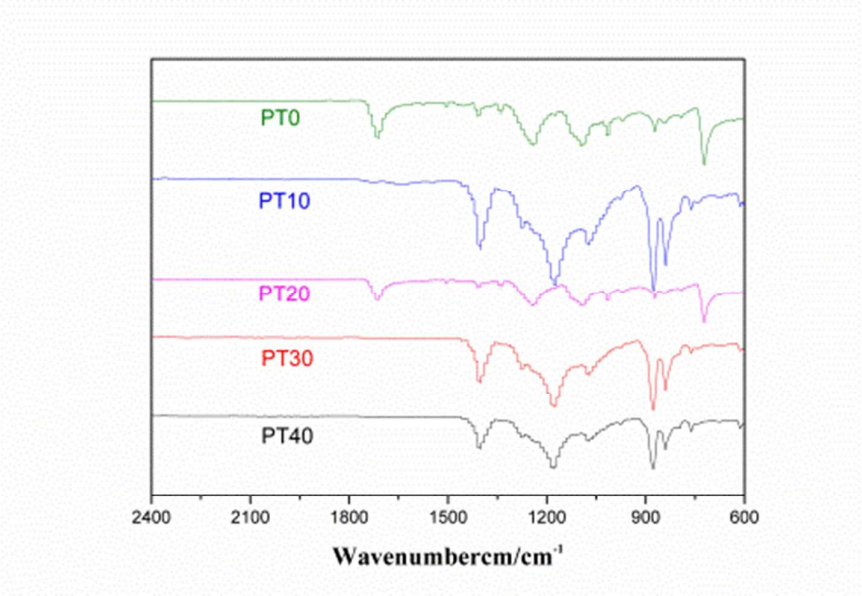

Fig. 1 FTIR spectra of unfilled and hybrid membranes

3.2. XRD results

The microstructures of hybrid membranes (PT10, PT20, PT30 and PT40) and unfilled PVDF membranes (PT0) were studied with XRD analysis. The results were presented in Fig. 2, where the intensity of X-Ray scattering was plotted against the diffraction angle denoted as 2θ. As seen in Fig. 2, PT0 was a type of semi crystalline polymer to show diffraction peaks at 2θ=20° and 36° due to the existence of form□crystals of ferroelectric all-trans phase. Compared with PT0, diffraction peak

at 2θ=18° occurred in PT30 and PT40, which corresponded to α crystalline phase of PVDF [36]. Besides, diffraction peak at 2θ=26°, which was characteristic of α crystalline phases of PVDF, turned much stronger as SiO_2 content increased. It could be concluded that the presence of silica changed the PVDF crystal formation, which had been proved by FTIR results. Although locations of corresponding hybrid peaks did not shift much due to the incorporation of silicate, the X-ray diffraction peak was broaden with a decrease in peak intensity as the silica content increased, which meant an increase of the amorphous region in the hybrid membranes. This indicated that stronger hydrogen bonding occurred in the hybrid membranes, which gave rise to the perturbation of long-ranged spacing between the chains [37]. Kim [38] investigated the hybrid membranes containing sulfonic acid groups and he found that the ascending SiO_2 content broadened the amorphous region in the hybrid membranes, which was consistent with those observed in this study.

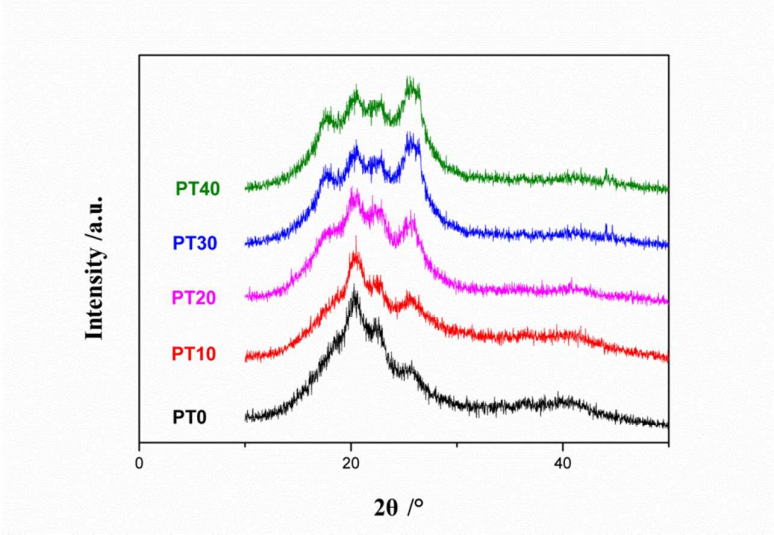

Fig. 2 XRD patterns of unfilled and hybrid membranes

3.3. Thermal and mechanical properties

The DSC endothermic curves of hybrid membranes (PT10, PT20, PT30 and PT40) and unfilled PVDF membranes (PT0) were shown in Fig. 3. The corresponding thermal data were listed in Table 1.The melting temperature increased with higher TEOS content, but the intensity of peak decreased. The degree of crystallinity [39, 40] could be determined from Eq. (9):

$$X = \frac{\Delta H_m}{\Phi \Delta H_m^0} \times 100\% \quad (9)$$

where X is the degree of crystallinity, Φ is the PVDF content in hybrids by weight fraction, ΔH_m and ΔH_m° are the experimental heat of fusion and the equilibrium heat of fusion for complete

PVDF crystals, respectively. ΔH_m° for PVDF was 104 J/g in this study. The results were shown in Table 1. The phenomena that the crystallinity decreased with the increasing TEOS content was attributed to the introduction of amorphous SiO_2 into the hybrid membranes. It was consistent with the results of XRD analysis.

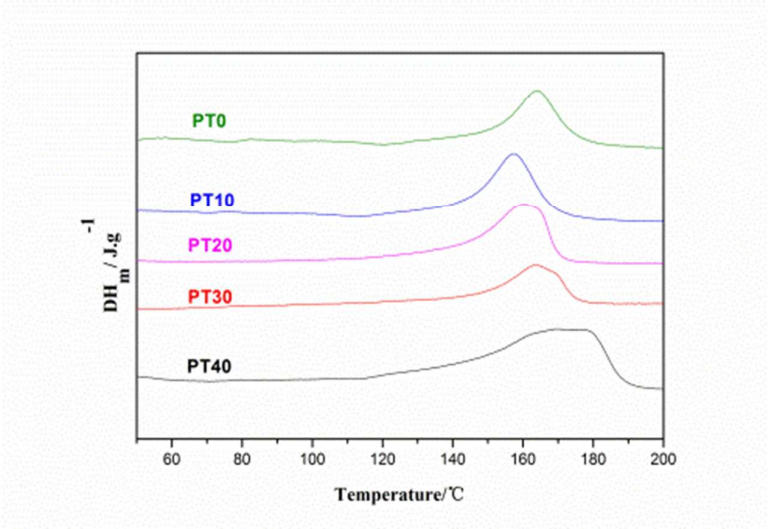

Fig. 3 DSC thermograms of unfilled and hybrid membranes

Table 1 Thermal data of unfilled and hybrid membranes

Membrane	Melting temperature (T_m, ℃)	Heat of fusion (ΔH_m, J/g)	Crystallinity (X, %)
PT0	163.0	30.23	29.1
PT10	163.4	25.32	24.3
PT20	165.5	20.86	20.1
PT30	166.0	20.66	19.9
PT40	176.0	17.77	17.8

The changing tendency of residual weight of hybrid membranes (PT10, PT20, PT30 and PT40) and unfilled PVDF membrane (PT0) with temperature was tested to investigate their thermal stability and the analytical results were shown in Fig. 4. There existed major weight loss of all membranes from 400 □ due to the decomposition of the polymer. The decomposition temperature slightly increased with rising TEOS content. Besides, it could be also seen that the weight residue of the membranes increased with the climbing TEOS content after 550 □. The improvement in thermal stability of hybrid membranes contributed to the inhibition of SiO_2 immobilized in the polymer by

silica cages.

Tensile evaluation was performed on hybrid membranes (PT10, PT20, PT30 and PT40) as well as unfilled PVDF membrane (PT0) and the analytical results were showed in Fig. 5 and Table 2. As indicated in Table 2, the tensile strength, elongation at break and Young's modulus all increased as TEOS content increased up to 30%, but decreased when TEOS content reached 40%. The phenomena were explained as follows. When TEOS content was lower than 30%, SiO_2 generated was dispersed evenly in polymer matrix and the PVDF chain interacted strongly with SiO_2 or silanol through hydrogen bonding [41, 42] consequently becoming entrapped between silica precipitates. Thus, SiO_2 could act as a crosslinking point in hybrid membranes and increase the rigidity of polymeric chains, so the mechanical properties could be improved with silica formation. However, at higher TEOS content of 40%, the formed superfluous silica particles in PVDF increased the rigidness of membrane and confined the crystallization of PVDF, which finally led to the decrease of the mechanical properties.

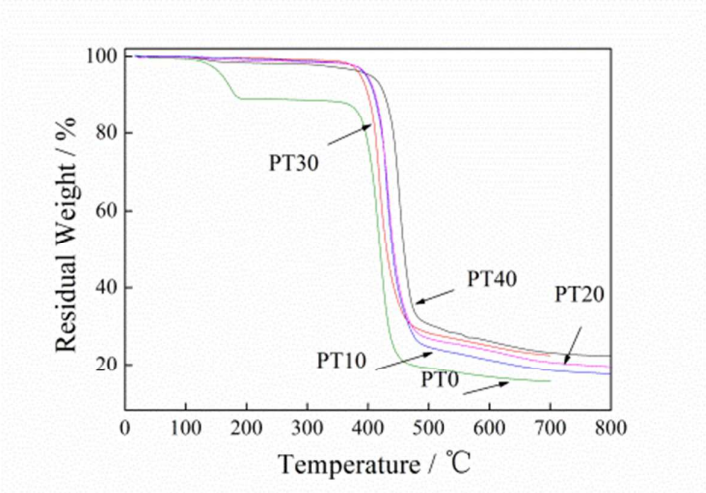

Fig.4 TGA curves of unfilled and hybrid membranes

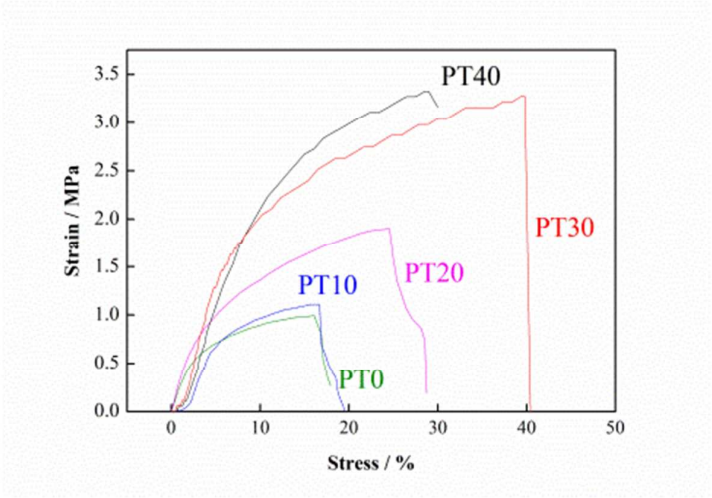

Fig.5 Stress-strain curves of unfilled and hybrid membranes

Table 2 Mechanical properties of unfilled and hybrid membranes

Membranes	Tensile strength /MPa	Elongation at break /%	**Young's** modulus /MPa
PT0	0.90	18.20	24.388
PT10	1.07	18.54	25.549
PT20	1.89	28.65	34.585
PT30	3.48	40.25	37.443
PT40	3.32	30.15	29.862

3.4 AFM results

Fig. 6 indicated the three-dimensional AFM images for the surfaces of the hybrid membrane (PT20) and unfilled PVDF membranes (PT0) over 2 μm×2 μm scan size. In these images, the brightest area presented the highest point of the membrane surface and the dark regions indicated valleys or membrane pores. The roughness parameters of the membrane surfaces were calculated by AFM software and were presented in Table 3.

The surface roughness of PT20 membrane was apparently higher than that of PT0. PT0 membrane had the smoothest surface. According to the classical theory, higher roughness could be assigned to higher porosity of the external surface of membranes, which led to two changes in the hybrid membrane: one was an increase of efficient filtration area and another was a decrease of the antifouling performance [43]. Due to the introduction of SiO_2 particles, the roughness and hydrophilicity of membrane surface increased, as a consequence, surface contamination could be

alleviated. Moreover, the adsorbed foulants on the membrane surface and pore wall could be more easily removed by shear force than those on pure PVDF membranes. Thus the increased membrane surface roughness did not have negative impact on membrane performance but improved the anti-fouling properties. Yan [44] studied the effect of the addition of nano-sized Al_2O_3 particle on PVDF ultrafiltration membrane performance and found that the addition of Al_2O_3 particle increased the membrane surface roughness, but it improved effectively the permeation flux and anti-fouling properties contrarily, which was in accordance with what had been proved in this paper.

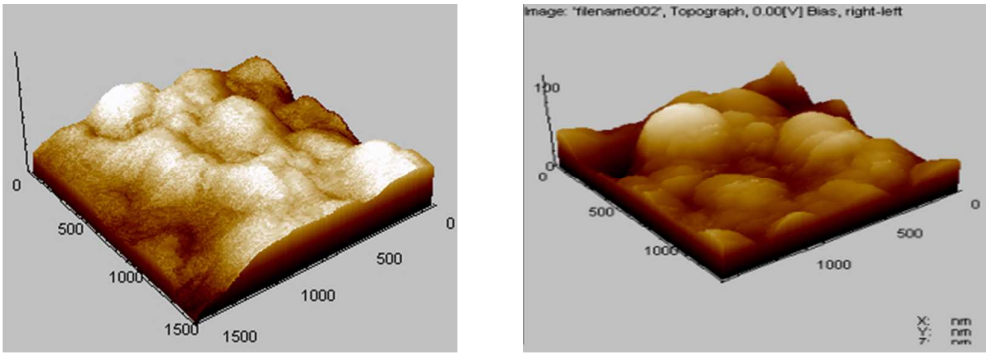

(a) (b)

Fig. 6 AFM three-dimensional surface images of PT0 (a) and PT20 (b) membranes

Table 3 Surface parameters of PT0 and PT20 membranes

Membranes	Roughness/nm		
	R_a*	R_q	R_{max}
PT0	15.0	17.8	101.4
PT20	66.2	184.7	348.5

* R_a , R_q and R_{max} are the mean roughness, the root mean square roughness and the maximal roughness, respectively.

3.5 Hydrophilicity, porosity and pore size

The surface hydrophilicity of membranes had great effects on the flux and anti-fouling property of membranes. In general, hydrophilicity was evaluated by water contact angle and higher hydrophilicity resulted from a smaller contact angle value. Fig. 7 revealed the effects of TEOS content on the water contact angle of hybrid membranes (PT10, PT20, PT30 and PT40) as well as unfilled PVDF membrane (PT0). The contact angles of all the hybrid membranes decreased with

the ascending TEOS content, which was attributed to the increasing amount of –OH groups on the SiO_2 particles generated by TEOS hydrolysis, as revealed by FTIR spectra in Fig. 1.

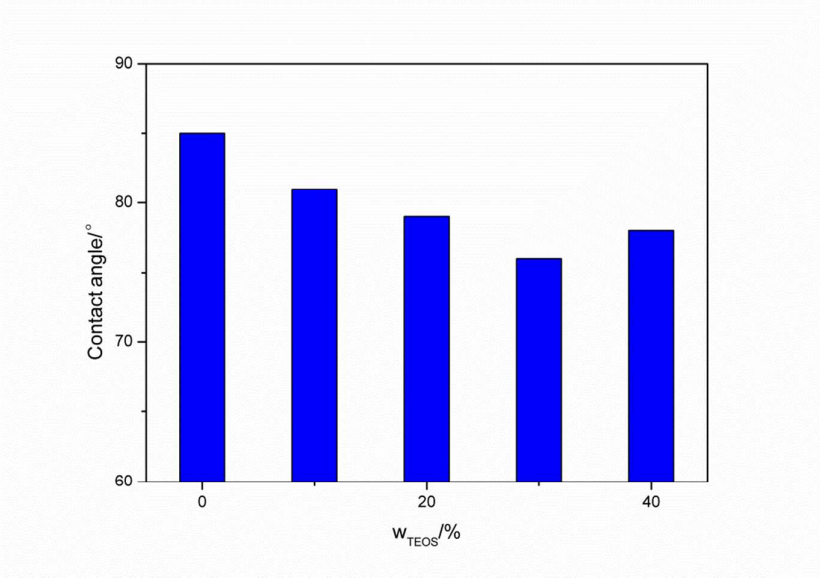

Fig. 7 The effects of TEOS content on the water contact angle values of membranes

Fig. 8 reflected the effects of TEOS content on the porosity and pore size of hybrid membranes (PT10, PT20, PT30 and PT40) as well as unfilled PVDF membrane (PT0). As demonstrated in Fig. 8, the porosity and pore size both increased with the TEOS content firstly and decreased afterwards. The results were explained as follows. TEOS hydrolysis polycondensation reaction produced water, which increased the content of non-solvent in casting solution and accelerated phase separation process. Thus the accumulation of the PVDF molecules was prevented effectively and membrane porosity was increased [45]. Meanwhile, SiO_2 generated by TEOS hydrolysis could increase the viscosity of the casting solution and slowed down phase separation process, which contributed to the accumulation of the PVDF molecules and prevented the formation of large pores. Accordingly the hybrid membrane pores turned more compact.

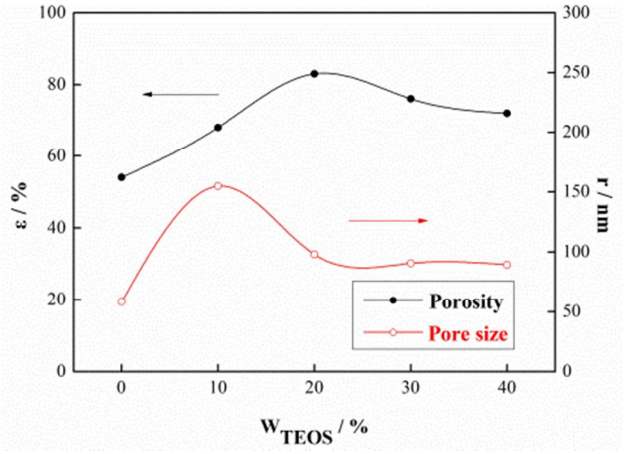

Fig. 8 The effects of TEOS content on porosity and pore size of membranes

3.6 Permeation flux and rejection rate

Fig. 9 indicated that the effects of TEOS content on the separation performance of hybrid membranes (PT10, PT20, PT30 and PT40) as well as unfilled PVDF membrane (PT0). As seen in Fig. 9, the pure water flux and rejection rate both increased with TEOS content firstly and decreased afterwards. There existed a maximal peak value of 2842.1 $L \cdot m^{-2} \cdot h^{-1}$ for pure water flux using PT10 membrane and a highest peak value of 94% for rejection rate using PT20 membrane. The phenomena could be explained as follows. The increase in the membrane hydrophilicity and mean pore size based on the lower TEOS content could attract water molecules inside the membrane matrix, which resulted in their penetration through the membrane and enhanced permeability. However, higher TEOS content slowed down the formation process of hybrid membranes and produced a denser sublayer, thereby decreasing the mean pore size and resulting in the decrease in permeability.

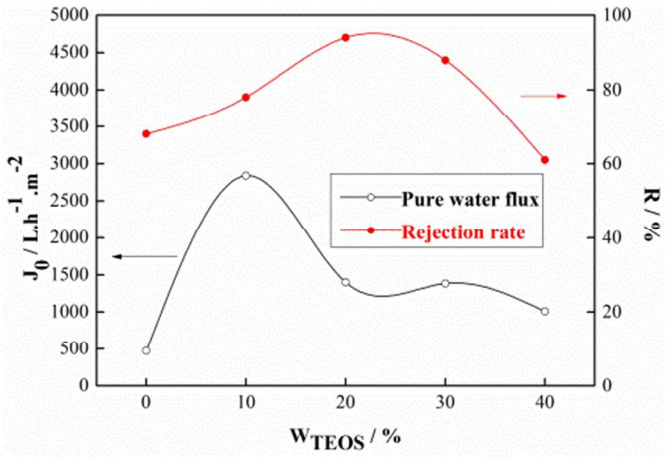

Fig. 9 The effects of TEOS content on pure water flux and rejection rate of membranes

3.7 Flux recovery

Fig. 10 reflected the water flux recovery of hybrid membranes (PT10, PT20, PT30 and PT40) as well as unfilled PVDF membrane (PT0) after BSA ultrafiltration process. As seen in Fig. 10, the water flux recovery increased with TEOS content and decreased afterwards. At TEOS content of 20%, the water flux recovery reached a maximum value of 95%. This could be explained by the influence of hydrophilicity and roughness of membrane surface on the water flux recovery. Due to the proper addition amount of SiO_2, a hydrophilic membrane surface layer was formed, which resulted in an excellent anticoagulation layer. However, the surface roughness of hybrid membranes with extortionate TEOS content was much serious, which brought about that the impurities cut-off was not cleared easily.

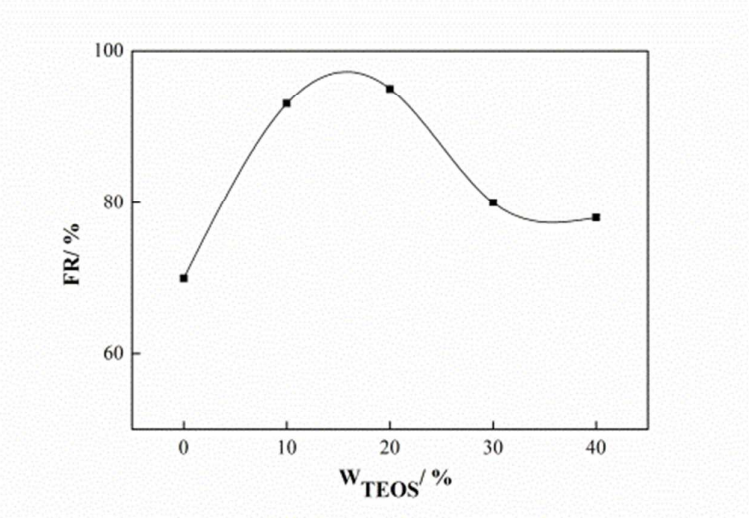

Fig. 10 The influence of TEOS content on water flux recovery of membranes

3.8 Ultrafiltration results of fennel oil in water extract

The effects of TEOS contents on removal rate of COD of hybrid membranes (PT10, PT20, PT30 and PT40) as well as unfilled PVDF membrane (PT0) were displayed in Fig. 11. As shown in Fig. 11, removal rate of COD of hybrid membranes increased with TEOS content firstly and decreased afterwards. Besides, removal rate of COD through PT20 reached a highest value of 68% while that through PT0 was only 50%. This changing tendency was in accordance with that of rejection rate of BSA with TEOS contents.

The dependence of water flux containing fennel oil through the hybrid membranes (PT10, PT20, PT30 and PT40) as well as unfilled PVDF membrane (PT0) on treatment time was

demonstrated in Fig. 12. It was found that water flux containing fennel oil though PT20 descended with treatment time and tended towards stability after 150 minutes to reach 700 $L \cdot m^{-2} \cdot h^{-1}$, while that through PT0 at stable condition was 360 $L \cdot m^{-2} \cdot h^{-1}$.

By overall comparison of removal rate of COD in Fig. 11 and water flux containing fennel oil in Fig. 12, the experimental results had proved that concentration performance of fennel oil in water extract was effectively improved due to the proper introduction of SiO_2.

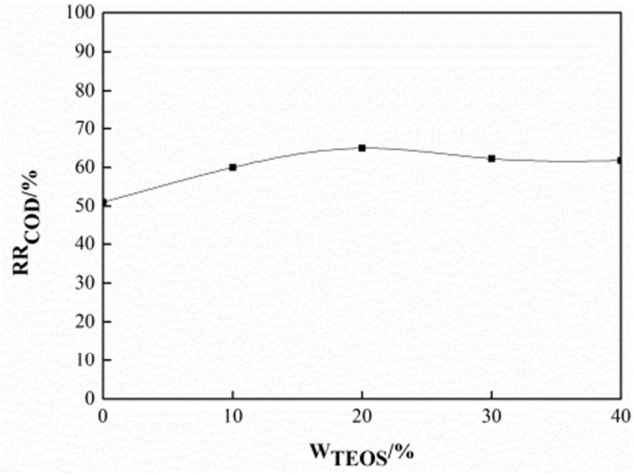

Fig. 11 The influence of TEOS content on COD removal rate of membranes

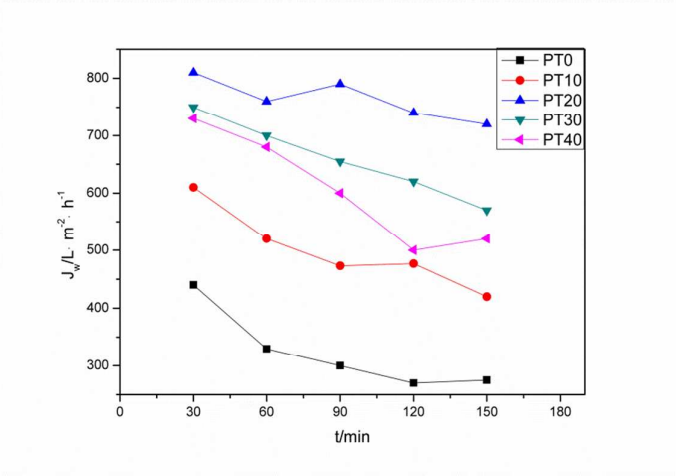

Fig. 12 The dependence of water flux containing fennel oil through membranes on time

4. Conclusions

Organic-inorganic PVDF/SiO_2 ultrafiltration membranes were prepared by a TEOS **sol-gel** method for the concentration of fennel oil in water extract. The hybrid membranes were characterized in terms of crystal structure, mechanical properties, thermal stability, morphology,

hydrophilicity, and permeation performance. The thermal and mechanical properties of the hybrid membrane were improved by the proper introduction of SiO_2. The crystalline structure of PVDF changed from β phase to α phase when TEOS content surpassed 20%. The hybrid membranes exhibited excellent permeability and rejection rate as well as anti-fouling properties compared with PVDF membrane. Besides, the concentration process of fennel oil in herbal water extract by hybrid membranes was carried on and it proved that separation performance was effectively improved.

Acknowledgements

This work was financially supported by the National Natural Scientific Funds of China (No. 81274095) and Natural Scientific Funds of Jiangsu Province of China (BK2012727).

References

[1] Y.S. Li, L. Yan, C.B. Xiang, L.J. Hong, Treatment of oily wastewater by organic－inorganic composite tubular ultrafiltration (UF) membranes, Desalination 196(2006) 76－83.

[2] W. Chen, Y. Su, L. Zheng, L. Wang, Z. Jiang, The improved oil/water separation performance of cellulose acetate-graft-polyacrylonitrile membranes, J. Membr. Sci.337 (2009) 98－105.

[3] L. Li, L. Dinga, Z. Tua, Y. Wanb, D. Claussea, J.-L. Lanoiselléa, Recovery of linseed oil dispersed within an oil-in-water emulsion using hydrophilic membrane by rotating disk filtration system, J. Membr. Sci. 342 (2009) 70－79.

[4]W. Chen, J. Peng, Y. Su, L. Zheng, L. Wang, Z. Jiang, Separation of oil/water emulsion using Pluronic F127 modified polyethersulfone ultrafiltration membranes, Sep. Purif. Technol. 66 (2009) 591－597.

[5] S. Simone, A. Figoli, A. Criscuoli, M.C. Carnevale, A. Rosselli, E. Drioli, Preparation of hollow fibre membranes from PVDF/PVP blends and their application in VMD, J. Membr. Sci., 364 (2010) 219-232.

[6] A.H. Cui, Z. Liu, C.F. Xiao, Y.F. Zhang, Effect of micro-sized SiO2-particle on the performance of PVDF blend membranes via TIPS, J. Membr. Sci., 360 (2010) 259-264.

[7] X.X. Yang, B. Deng, Z.Y. Liu, L.Q. Shi, X.K. Bian, M. Yu, L.F. Li, J.Y. Li, X.F. Lu, Microfiltration membranes prepared from acryl amide grafted poly(vinylidene fluoride) powder and their pH sensitive behaviour, J. Membr. Sci., 362 (2010) 298-305.

[8] C.X. Mu, Y.L. Su, M.P. Sun, W.J. Chen, Z.Y. Jiang, Remarkable improvement of the performance of poly(vinylidene fluoride) microfiltration membranes by the additive of cellulose acetate, J. Membr. Sci., 350 (2010) 293-300.

[9] Y.M. Zheng, S.W. Zou, K.G.N. Nanayakkara, T. Matsuura, J.P. Chen, Adsorptive removal of arsenic from aqueous solution by a PVDF/zirconia blend flat sheet membrane, J. Membr. Sci., 374 (2011) 1-11.

[10] F. Liu, N.A. Hashim, Y.T. Liu, M.R.M. Abed, K. Li, Progress in the production and modification of PVDF membranes, J. Membr. Sci., 375 (2011) 1-27.

[11] Y.C. Chiang, Y. Chang, A. Higuchi, W.Y. Chen, R.C. Ruaan, Sulfobetaine-grafted poly(vinylidene fluoride) ultrafiltration membranes exhibit excellent antifouling property, J. Membr. Sci., 339 (2009) 151-159.

[12] X.T. Zuo, S.L. Yu, X. Xu, J. Xu, R.L. Bao, X.J. Yan, New PVDF organic-inorganic membranes: The effect of SiO2 nanoparticles content on the transport performance of anion-exchange membranes, J. Membr. Sci., 340 (2009) 206-213.

[13] H.L. Shen, H. Liao, C.F. Xiao, Formation Mechanism and Properties of Polyvinylidene Fluoride (PVDF)/nano-silica Hybrid Membranes, in: Multi-Functional Materials And Structures Iii, Pts 1 And 2, Trans Tech Publications Ltd, Stafa-Zurich, pp. 93-96.

[14] P. Andry, A.Y. Filion, S. Blain, A. Rambo, L.G. Caron, Inversion Induced In Silicon By Corona-Charged Pvdf, P(Vdf/Trife), And P(Vdf/Citrife), J. Appl. Phys., 69 (1991) 2644-2655.

[15] M. Caillon-Caravanier, B. Claude-Montigny, D. Lemordant, G. Bosser, Absorption ability and kinetics of a liquid electrolyte in PVDF-HFP copolymer containing or not SiO2, J. Power Sources, 107 (2002) 125-132.

[16] A. Bottino, G. Capannelli, A. Comite, Preparation and characterization of novel porous PVDF-ZrO2 composite membranes, Desalination, 146 (2002) 35-40.

[17] F. Liu, M.R.M. Abed, K. Li, Preparation and characterization of poly(vinylidene fluoride) (PVDF) based ultrafiltration membranes using nano gamma-Al2O3, J. Membr. Sci., 366 (2011) 97-103.

[18] S.J. Oh, N. Kim, Y.T. Lee, Preparation and characterization of PVDF/TiO2 organic-inorganic composite membranes for fouling resistance improvement, J. Membr. Sci., 345 (2009) 13-20.

[19] R.A. Damodar, S.J. You, H.H. Chou, Study the self cleaning, antibacterial and photocatalytic properties of TiO2 entrapped PVDF membranes, Journal Of Hazardous Materials, 172 (2009)

1321-1328.

[20] J. Dulebohn, P. Ahmadiannamini, T. Wang, S. S. Kim, T. J. Pinnavaia, V. V. Tarabara. Polymer mesocomposites: Ultrafiltration membrane materials with enhanced permeability, selectivity and fouling resistance, J. Membr. Sci., 453 (2014) 478-488.

[21] S. H. Zhi, J. Xu, R. Deng, L.S. Wan, Z. K. Xu. Poly (vinylidene fluoride) ultrafiltration membranes containing hybrid silica nanoparticles: Preparation, characterization and performance, Polymer, 55(2014) 1333-1340.

[22] A. Martín, J. M. Arsuaga, N. Roldán, J. de Abajo, A. Martínez, A. Sotto. Enhanced ultrafiltration PES membranes doped with mesostructured functionalized silica particles, Desalination, 357 (2015) 16-25.

[23] J.W. Park, Y.A. Seo, C.S. Ha, Investigating the crystalline structure of poly(vinylidene fluoride)(PVDF) in PVDF/silica binary and PVDF/poly(methyl methacrylate)/silica ternary hybrid composites using FTIR and solid-state ^{19}F MAS NMR spectroscopy, Macromolecules 37 (2004) 429 – 436.

[24] J.W. Cho, K.I. Sul, Characterization and properties of hybrid composites prepared frompoly(vinylidene fluoride-tetrafluoroethylene) and SiO2, Polymer 42 (2001) 727 – 736.

[25] R.A. Zoppi, C.G.A. Soares, Hybrids of poly(ethylene oxide-b-amide-6) and ZrO2 sol – gel: preparation, characterization, and application in processes of membrane separation, Adv. Polym. Technol. 21 (2002) 2 – 16.

[26] R.K. Nagarale, V.K. Shahi, R. Rangarajan, Preparation of polyvinyl alcohol – silica hybrid heterogeneous anion-exchangemembranes by sol – gelmethod and their characterization, J. Membr. Sci. 248 (2005) 37 – 44.

[27]X.J. Liu, Y.L. Peng, S.L. Ji, A new method to prepare organic-inorganic hybrid membranes, Desalination, 221 (2008) 376-382.

[28] Q. Li, Z.L. Xu, L.Y. Yu, Effects of Mixed Solvents and PVDF Types on Performances of PVDF Microporous Membranes, J. Appl. Polym. Sci., 115 (2009) 2277-2287.

[29] E.S. Kim, Y.J. Kim, Q.S. Yu, B.L. Deng, Preparation and characterization of polyamide thin-film composite (TFC) membranes on plasma-modified polyvinylidene fluoride (PVDF), J. Membr. Sci., 344 (2009) 71-81.

[30] Z.H. Xu, L. Li, F. W. Wu, S. J. Tan, Z. B. Zhang, The application of the modified PVDF ultrafiltration membranes in further purification of Ginkgo biloba extraction, J. Membr. Sci.

255(2005) 125 – 131.

[31] T. Berrin, R. Jayadev, S. Robert, Treatment of fuel oil and crude oil contaminated waters ultrafiltration membranes, Desalination, 102 (1995) 301-311.

[32] M. Touzin, F. Beclin, Fabrication and characterization of composite sol-gel coatings on porous ceramic substrate, J. Eur. Ceram. Soc., 31(2008)1661-1667.

[33] J.W. Kim, W.J. Cho, C.S. Ha, Morphology, crystalline structure, and properties of poly(vinylidene fluoride)/silica hybrid composites, J. Polym. Sci. Pt. B-Polym. Phys., 40 (2002) 19-30.

[34] J. Buckley, P. Cebe, D. Cherdack, e. al, Nanocomposite of poly (vinylidene fluoride) with organically modified silicate, PolymER, 47 (2006) 11.

[35] J.W. Park, Y.A. Seo, I. Kim, C.S. Ha, K. Aimi, S. Ando, Investigating the crystalline structure of poly(vinylidene fluoride) (PVDF) in PVDF/silica binary and PVDF/poly(methyl methacrylate)/silica ternary hybrid composites using FTIR and solid-state F-19 MAS NMR spectroscopy, Macromolecules, 37 (2004) 429-436.

[36] L.Y. Yu, Z.L. Xu, H.M. Shen, H. Yang, Preparation and characterization of PVDF-SiO2 composite hollow fiber UF membrane by sol-gel method, J. Membr. Sci., 337 (2009) 257-265.

[37] S. Wen, C.L. Gong, W.C. Tsen, Y.C. Shu, F.C. Tsai, Sulfonated Poly(ether sulfone)/Silica Composite Membranes for Direct Methanol Fuel Cells, J. Appl. Polym. Sci., 116 (2010) 1491-1498.

[38] D.S. Kim, H.B. Park, Y.M. Lee, Y.H. Park, J.W. Rhim, Preparation and characterization of PVDF/silica hybrid membranes containing sulfonic acid groups, J. Appl. Polym. Sci., 93 (2004) 209-218.

[39] J.W. Cho, K.I. Sul, Crystallization of poly (vinylidene fluoride)-SiO 2 hybrid composites prepared by a Sol-gel process, Fibers and Polymers, 2 (2001) 135-140.

[40] Y.H. Zhao, Y.Y. Xu, B.K. Zhu, In Situ Crosslinking of Hyperbranched Polyglycerol in Casting Solutions and Its Effect on the Structure and Properties of Porous PVDF Membranes, J. Appl. Polym. Sci., 117 (2010) 548-556.

[41] S. Yano, K. Iwata, K. Kurita, Physical properties and structure of organic-inorganic hybrid materials produced by sol-gel process, Materials Science and Engineering: C, 6 (1998) 75-90.

[42] D.K. Roh, J.K. Choi, J.K. Koh, Y.G. Shul, J.H. Kim, Nanocomposite proton conducting membranes based on amphiphilic PVDF graft copolymer, Macromol. Res., 18 (2010) 271-278.

[43] L.Y. Yu, H.M. Shen, Z.L. Xu, PVDF–TiO2 composite hollow fiber ultrafiltration membranes

prepared by TiO2 sol–gel method and blending method, J. Appl. Polym. Sci., 113 (2009) 1763-1772.

[44] L. Yan, Y.S. Li, C.B. Xiang, S. Xianda, Effect of nano-sized Al2O3-particle addition on PVDF ultrafiltration membrane performance, J. Membr. Sci., 276 (2006) 162-167.

[45] H. Q. Yu, Y. H. Li, H. J. Zhao, Preparation and characterization of SiO_2/PSf organo-mineral composite ultrafiltration membrane, Membrane science and technology, 30(2010) 29-33.

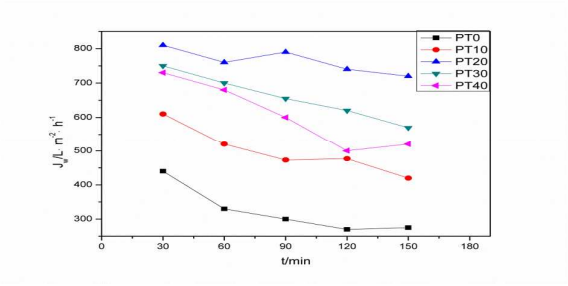

PVDF/SiO_2 membranes by sol-gel were characterized and ultrafiltration performance of fennel oil in water extract through them was effectively improved.